

# A Two-Stage Framework for Multiple Sound-Source Localization

Rui Qian<sup>1</sup>, Di Hu<sup>2</sup>, Heinrich Dinkel<sup>1</sup>, Mengyue Wu<sup>1</sup>, Ning Xu<sup>3</sup>, Weiyao Lin<sup>1</sup>  
<sup>1</sup>Shanghai Jiao Tong University, <sup>2</sup>Baidu Research, <sup>3</sup>Adobe Research

## 1. Introduction

Humans usually perceive the world through information in different modalities, *e.g.*, vision and hearing. By leveraging the relevance and complementary between audio and vision, humans can clearly distinguish different sound sources and infer which object is making sound. In contrast, machines have been proven capable of separately processing audio and visual information using deep neural networks. But can they benefit from joint audiovisual learning?

Recent works mainly focus on establishing multi-modal relationship based on temporally synchronized audio and visual signals [1, 3, 8]. This synchronization works effectively for simple scenes [2, 9], *i.e.*, the single-source conditions. However, in unconstrained videos, various sounds are usually mixed, where the scene-level supervision is too coarse to provide the precise alignment between each sound and visual source pair. To tackle this problem, [6, 7] establish audiovisual clusters to associate sound-object pairs, but require pre-determined number of clusters, which is difficult in unconstrained scenarios, thus greatly affecting alignment performance. [2, 9, 11] further apply audiovisual learning into sound localization, but mainly focus on simple scenes, usually unable to find source-specific objects from mixed audio. [13] constructs a pretext task then localizes sound through energy of each pixel.

To sum up, existing dominant methods mostly lack the ability to analyze complex audiovisual scenes, and fail to effectively utilize the latent alignment between sound and visual source pairs in unconstrained videos. This is because there are majorly two challenges in complex audiovisual scene analysis: one is how to distinguish different sound-sources, the other is how to ensure the established sound-object alignment is fairly satisfactory without one-to-one annotations. To address these challenges, we develop a two-stage audiovisual learning framework. At the first stage, we employ a multi-task framework consisting of classification and audiovisual correspondence to provide the reference of audiovisual content for the second stage. At the second stage, based on the classification predictions, we use the operation of *Class Activation Mapping* (CAM) [14, 10, 4] to extract class-specific feature representations as the potential sound-object pairs (Fig. 1), then perform alignment in

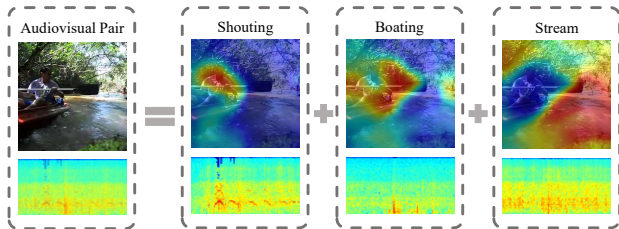


Figure 1. Our model separates a complex audiovisual scene into several simple scenes, which simplifies a complex scenario and generates several one-to-one audiovisual associations.

a coarse-to-fine manner, where the coarse correspondence based on category is evolved into the fine-grained matching in both video- and category-level.

Our main contributions can be summarized as follows: (1) We develop a two-stage audiovisual learning framework to deal with the complex scenes. (2) We propose to establish audiovisual alignment in a coarse-to-fine manner. (3) We achieve state-of-the-art results on public dataset. In the multi-source conditions, according to our proposed class-specific localization metric, our method shows considerable performance compared with several baselines.

## 2. Approach

Our two-stage framework is illustrated in Fig. 2. At the first stage, we adopt multi-task learning for classification and video-level audiovisual correspondence. At the second stage, we use Grad-CAM [10] modules to disentangle class-specific features on both modalities, based on which we further perform fine-grained audiovisual alignment.

### 2.1. Multi-Task Learning Framework

Given audio and visual (image) messages,  $\{a_i, v_i\}$  from  $i$ -th video, we use video tags or pseudo labels from pre-trained models as supervision for classification. We denote  $C$  as the number of class and  $c$  as the  $c$ -th class. Multi-label binary cross entropy loss is considered for classification:

$$L_{cls} = \mathcal{H}_{bce}(\mathbf{y}_{a_i}, \mathbf{p}_{a_i}) + \mathcal{H}_{bce}(\mathbf{y}_{v_i}, \mathbf{p}_{v_i}), \quad (1)$$

where  $\mathcal{H}_{bce}$  is the binary cross-entropy loss,  $\mathbf{y}$  and  $\mathbf{p}$  are the class labels and corresponding predicted probabilities

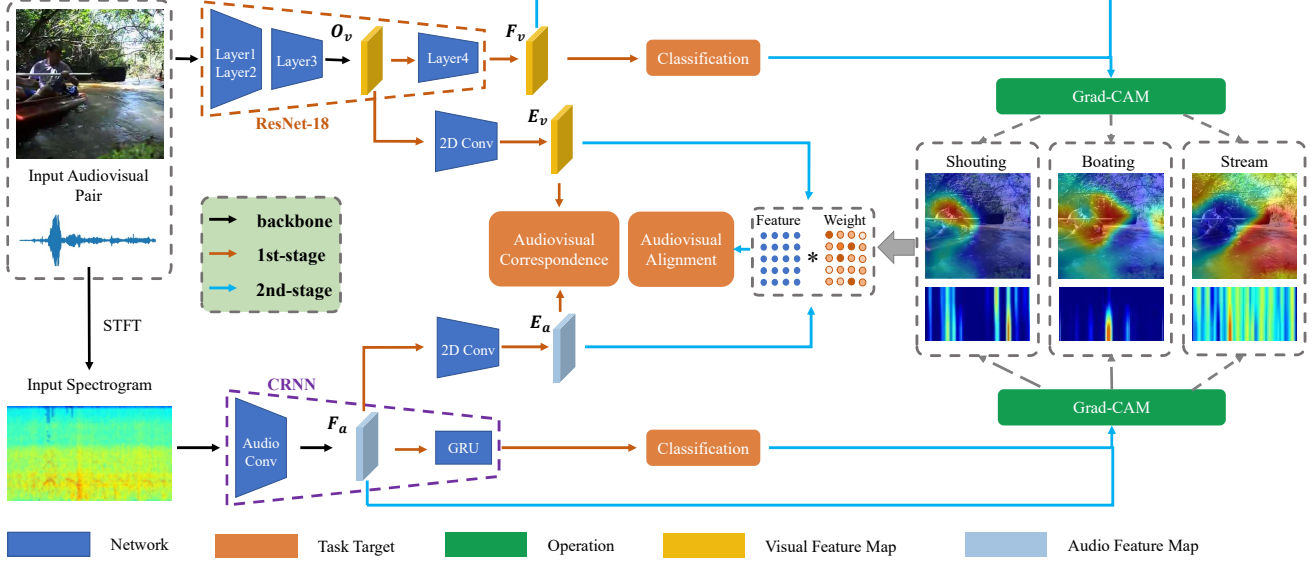


Figure 2. An overview of our two-stage audiovisual learning framework. At the first stage, the model performs classification and video-level correspondence. At the second stage, we disentangle class-aware representations and implement fine-grained audiovisual alignment.

respectively,  $\mathbf{y} \in \{0, 1\}^C$ ,  $\mathbf{p} \in [0, 1]^C$ .

For audiovisual correspondence learning, similar to [1], we view it as a two-class classification problem. Specifically, we take  $F_a$  and  $O_v$  in Fig. 2 as inputs<sup>1</sup> for audiovisual correspondence network. Through a series of convolutions and concatenation, we get one 1024-D vector and pass it through two fully-connected layers of 1024-128-2. The 2-D output with softmax regression aims to determine whether audio and vision correspond.  $\{a_i, v_i\}$  from  $i$ -th video are viewed as corresponding pair, the image of a randomly selected video,  $v_j$ , is used to construct mis-corresponding pair  $\{a_i, v_j\}$ . The learning objective can be written as:

$$L_{avc} = \mathcal{H}_{cce}(\delta, \mathbf{q}), \quad (2)$$

where  $\mathcal{H}_{cce}$  is the categorical cross entropy loss,  $\mathbf{q} \in [0, 1]^2$  is the predicted output,  $\delta$  is the class indicator,  $\delta = (0, 1)$  for correspondence while  $\delta = (1, 0)$  for not.

We take  $L_{mul}$  as final loss function for multi-task learning,  $\lambda$  is the hyperparameter of weighting:

$$L_{mul} = L_{cls} + \lambda L_{avc}. \quad (3)$$

After training with  $L_{mul}$ , we could achieve coarse-grained audiovisual correspondence in the category level.

## 2.2. Audiovisual Feature Alignment

In this section, we propose to disentangle feature representations of different categories and implement fine-grained audiovisual alignment.

<sup>1</sup>We choose  $F_a$  and  $O_v$  for two reasons: we can obtain more fine-grained local features and achieve easier training process.

### 2.2.1 Disentangle Features by Grad-CAM.

We leverage the operation of Grad-CAM [10] to perform disentangle class-specific features. For simplicity, we use  $r \in \{a, v\}$  to represent audio or visual modality. Given the feature map activations of the last convolutional layer,  $F_r$ , and the output of classification branch without activation for class  $c$ ,  $\hat{p}_r^c$ , we calculate the class-specific map  $W_r^c$ , i.e.,

$$W_r^c = \text{Grad-CAM}(F_r, \hat{p}_r^c). \quad (4)$$

Then we take  $W_r^c$  as weights to perform weighted global pooling over the feature map  $E_r(u, v)$  to obtain class-aware representation<sup>2</sup>, where  $u$  and  $v$  are the map entries. That is:

$$f_r^c = \frac{\sum_{u,v} E_r(u, v) W_r^c(u, v)}{\sum_{u,v} W_r^c(u, v)}. \quad (5)$$

Finally, we get  $C$  512-D vectors as the feature representation of all the categories.  $\{f_{a_i}^m | m = 1, 2, \dots, C\}$  and  $\{f_{v_i}^n | n = 1, 2, \dots, C\}$  are the set of audio and visual class-specific feature representations for  $i$ -th video.

### 2.2.2 Fine-Grained Audiovisual Alignment.

To establish audiovisual alignment with disentangled features, we take pairs of the same class from the same video as positive pairs for alignment. As each category contains various entities (e.g., the animal category contains audio and visual patterns of dogs, cats, birds etc.), with this sampling

<sup>2</sup>We find that directly using  $F_r$  with the weights  $W_r^c$  is difficult to perform alignment objective, but by performing weighted pooling on  $E_r$ , we achieve easier training and faster convergence.

strategy, we could acquire higher-quality positive pairs and establish sound-object association beyond category.

To establish cross-modality alignment, we project  $f_{a_i}^m$  and  $f_{v_j}^n$  into a shared embedding space via two fully-connected layers of 512-128-128. Then we compare the projected features using Euclidean distance,

$$D(f_{a_i}^m, f_{v_j}^n) = \|g_a(f_{a_i}^m) - g_v(f_{v_j}^n)\|_2, \quad (6)$$

where  $g_a$  and  $g_v$  are the fully-connected layers. We then adopt contrastive loss to perform sound-object alignment. The loss function is written as<sup>3</sup>

$$L_{ava} = \sum_{i,j=1}^N \sum_m \sum_n (\delta_{i=j}^{m=n} D^2(f_{a_i}^m, f_{v_j}^n) + (1 - \delta_{i=j}^{m=n}) \max(\Delta - D(f_{a_i}^m, f_{v_j}^n), 0)^2), \quad (7)$$

where  $\delta_{i=j}^{m=n}$  indicates whether the audiovisual pair is positive, *i.e.*,  $\delta_{i=j}^{m=n} = 1$  when  $i = j$  and  $m = n$ , otherwise 0.  $\Delta$  is a margin hyper-parameter.

### 2.3. Visual Localization of Sounds.

We use learned representations to visually localize sounds by generating source-aware localization maps. To leverage the established alignment, the visual feature map  $E_{v_i}$  of testing image is firstly projected into the shared embedding space via the fully-connected layers of  $g_v$  in Eq. 6, then compared with the disentangled  $c$ -th class audio features  $f_{a_i}^c$  through Eq. 8,

$$K_i^c(u, v) = \|g_a(f_{a_i}^c) - g_v(E_{v_i})(u, v)\|_2. \quad (8)$$

The obtained  $K_i^c \in \mathbb{R}^{U \times V}$  is then normalized and resized to the original image size as the final localization maps for sound source in the  $c$ -th class.

## 3. Experiments

In this work, we train and evaluate our model on SoundNet-Flickr [3], AudioSet-instrument [5], and also show some qualitative examples on AVE dataset [12].

### 3.1. Sound Localization on SoundNet-Flickr

We implement quantitative evaluation on 249 audiovisual pairs in the subset of SoundNet-Flickr used in [11]. Consensus Intersection over Union (cIoU) and Area Under Curve (AUC) [11] are reported. We use weighted summation over class-specific localization maps of valid categories as final results, where the weights are normalized predicted probabilities. Table 1 shows the results of different methods. Despite that most audiovisual pairs in test set are of single-source, our model still outperforms all the other methods including CAM results from the first stage. It demonstrates that our fine-grained alignment effectively facilitates audiovisual learning in unconstrained videos.

<sup>3</sup>In practice, a threshold is considered to select valid categories.

Table 1. Quantitative localization results on SoundNet-Flickr.

| Methods          | cIoU@0.5    | AUC         |
|------------------|-------------|-------------|
| Random           | 7.2         | 30.7        |
| Attention[11]    | 43.6        | 44.9        |
| DMC AudioSet[6]  | 41.6        | 45.2        |
| CAVL AudioSet[7] | 50.0        | 49.2        |
| Ours CAM         | 44.2        | 48.1        |
| Ours             | <b>52.2</b> | <b>49.6</b> |

Table 2. Quantitative results on AudioSet. The cIoU\_class threshold is 0.5 for level-1 and level-2, and 0.3 for level-3. Note that †AVC method is evaluated in a class-agnostic way.

| Methods    | level-1     |             | level-2     |             | level-3     |             |
|------------|-------------|-------------|-------------|-------------|-------------|-------------|
|            | cIoU_c      | AUC         | cIoU_c      | AUC         | cIoU_c      | AUC         |
| †AVC       | 24.8        | 32.0        | 4.27        | 23.6        | 5.3         | 14.9        |
| Multi-task | 20.6        | 29.5        | 2.37        | 17.4        | 10.5        | 17.8        |
| Ours       | <b>32.8</b> | <b>38.3</b> | <b>6.16</b> | <b>23.9</b> | <b>21.1</b> | <b>22.0</b> |

### 3.2. Multi-Source Localization on AudioSet

To better evaluate sound localization performance in multi-source scenes, we propose to use cIoU and AUC metric in a class-aware manner. We use the detected bounding boxes with category labels of Faster RCNN to indicate the localization of sounding objects<sup>4</sup>. Next, we calculate cIoU scores on each valid sound source and take an average. Final cIoU\_class on each frame can be calculated by

$$\text{cIoU\_class} = \frac{\sum_{c=1}^C \theta_c \text{cIoU}_c}{\sum_{c=1}^C \theta_c}, \quad (9)$$

where  $c$  indicates the class index of instruments,  $\theta_c = 1$  if instrument of class  $c$  makes sounds, otherwise 0.

We compare with two baselines: (1) AVC: only using video-level audiovisual correspondence, and inferring the sound locations in a class-agnostic way. (2) Multi-task learning: using both of classification and audiovisual correspondence. We report results on three difficulty levels, *i.e.*, single-source (level-1), two-source (level-2) and three-source (level-3), in Table 2, and there are several observations. First, localizing sound in a class-agnostic way is effective with limited sounding objects, but fails with more sources. This is because the video-level correspondence is too coarse to provide sound-object association in complex scenes. Second, although AVC takes a much looser evaluation metric of class-agnostic, it is still worse than the multi-task method on level-3, which reveals classification significantly helps to distinguish sounds of different sources. Third, our method significantly outperforms two baselines and is robust on all difficulty levels. It demonstrates that our fine-grained alignment is effective to establish one-to-one association in both single-source and multi-source scenes.

<sup>4</sup>We have filtered out those silent detected objects.

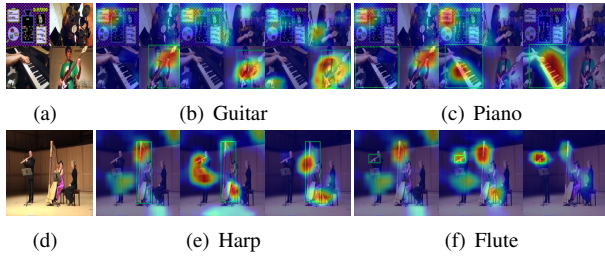


Figure 3. Some examples in AudioSet level-2. The localization maps in each subfigure are listed from left to right: AVC, Multi-task, Ours. The green boxes are detection results of Faster RCNN.

Some examples for the scenes in level-2 w.r.t. three different methods, AVC, Multi-task and Ours, are shown in Fig. 3. The results show our method can accurately associate sounds with specific instruments. For example, our model precisely focuses on the tiny area where the flute locates, while the other two associate flute sound with visual object of harp.

### 3.3. Comparison with CAM

In this subsection, we compare our method with category-level CAM output at the first stage. Concretely, we adopt the model trained on AVE dataset for comparison. Our model generates localization results following the procedure mentioned in the paper, while for CAM method, we adopt classification predictions on audio as prior, and generate class activation maps on visual modality.

As is shown in Fig. 4, CAM method cannot distinguish the objects belonging the same category, *e.g.*, aeroplane and car in Fig. 4(c), violin and piano in Fig. 4(d), while our model can precisely localize the sounding object, which demonstrates the efficacy of our second stage alignment. Interestingly, in Fig. 4(a) and Fig. 4(b), in the scene with multiple guitars, with background music sound, our model focuses on the silent guitars hanging on the wall, while with the sound of the man playing guitar, it precisely localizes the guitar held by the man. It is probably because the sound of playing guitar usually coexists with the visual pattern of the interaction between human hands with guitar, while the background music is usually accompanied with individually placed music instruments.

## References

[1] R. Arandjelovic and A. Zisserman. Look, listen and learn. In *2017 IEEE International Conference on Computer Vision (ICCV)*, pages 609–617, Oct 2017. 1, 2

[2] R. Arandjelovic and A. Zisserman. Objects that sound. In *The European Conference on Computer Vision (ECCV)*, September 2018. 1

[3] Y. Aytar, C. Vondrick, and A. Torralba. Soundnet: Learning sound representations from unlabeled video. In *Advances in*

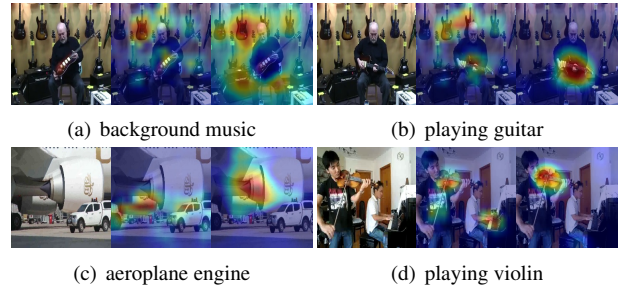


Figure 4. The images in each subfigure are listed as: original image, result of CAM method, result of our model. CAM method cannot distinguish the objects of the same category, *e.g.*, violin and piano in Fig. 4(d), but our model precisely focuses on the violin.

*Neural Information Processing Systems 29*, pages 892–900. Curran Associates, Inc., 2016. 1, 3

[4] A. Chattopadhyay, A. Sarkar, P. Howlader, and V. N. Balasubramanian. Grad-cam++: Generalized gradient-based visual explanations for deep convolutional networks. In *2018 IEEE Winter Conference on Applications of Computer Vision (WACV)*, pages 839–847, March 2018. 1

[5] R. Gao and K. Grauman. Co-separating sounds of visual objects. In *The IEEE International Conference on Computer Vision (ICCV)*, October 2019. 3

[6] D. Hu, F. Nie, and X. Li. Deep multimodal clustering for unsupervised audiovisual learning. In *The IEEE Conference on Computer Vision and Pattern Recognition (CVPR)*, June 2019. 1, 3

[7] D. Hu, Z. Wang, H. Xiong, D. Wang, F. Nie, and D. Dou. Curriculum audiovisual learning. *arXiv preprint arXiv:2001.09414*, 2020. 1, 3

[8] B. Korbar, D. Tran, and L. Torresani. Co-training of audio and video representations from self-supervised temporal synchronization. *ArXiv*, abs/1807.00230, 2018. 1

[9] A. Owens and A. A. Efros. Audio-visual scene analysis with self-supervised multisensory features. In *The European Conference on Computer Vision (ECCV)*, September 2018. 1

[10] R. R. Selvaraju, M. Cogswell, A. Das, R. Vedantam, D. Parikh, and D. Batra. Grad-cam: Visual explanations from deep networks via gradient-based localization. In *The IEEE International Conference on Computer Vision (ICCV)*, Oct 2017. 1, 2

[11] A. Senocak, T.-H. Oh, J. Kim, M.-H. Yang, and I. So Kweon. Learning to localize sound source in visual scenes. In *The IEEE Conference on Computer Vision and Pattern Recognition (CVPR)*, June 2018. 1, 3

[12] Y. Tian, J. Shi, B. Li, Z. Duan, and C. Xu. Audio-visual event localization in unconstrained videos. In *The European Conference on Computer Vision (ECCV)*, September 2018. 3

[13] H. Zhao, C. Gan, A. Rouditchenko, C. Vondrick, J. McDermott, and A. Torralba. The sound of pixels. In *The European Conference on Computer Vision (ECCV)*, September 2018. 1

[14] B. Zhou, A. Khosla, A. Lapedriza, A. Oliva, and A. Torralba. Learning deep features for discriminative localization. In *The IEEE Conference on Computer Vision and Pattern Recognition (CVPR)*, June 2016. 1